Int. J. Electrochem. Sci., 7 **(2012)** 8702 - 8712

International Journal of
ELECTROCHEMICAL
SCIENCE
www.electrochemsci.org

Electrochemically Enhanced Photocatalytic Degradation of Organic Pollutant on β-PbO_2-TNT/Ti/TNT Bifuctional Electrode

Yanming Shen[*], *Fei Li, Shifeng Li, Dongbin Liu, Lihui Fan, Yi Zhang*

School of Chemical Engineering, Shenyang University of Chemical Technolog, shenyang 110142, P.R. China
[*]E-mail: sym6821@sina.com.cn

Received: 25 July 2012 / *Accepted:* 12 August 2012 / *Published:* 1 September 2012

A bifunctional PbO_2-TNT/Ti/TNT electrode with both photo- and electro-catalytic performance was prepared. Firstly, TiO_2 nanotube (TNT) electrode was fabricated on the Ti foils by anodic oxidation and then deposited with β-PbO_2 on the reverse side of TNT electrode by electrodeposition. The obtained electrode was characterized by scanning electron microscopy (SEM), X-ray diffraction analysis (XRD) and cyclic voltammetry analysis (CV). Photoelectrocatalytic (PEC) performance of the bifunctional electrodes was investigated for the decolorization of methyl orange (MO). Compared with the Ti/TNT monofunctional electrode, the PbO_2-TNT/Ti/TNT bifunctional electrode shows higher PEC performance for the decolorization of MO, reaching 93% after 3 hr. The photoelectro-synergistic catalysis process on the PbO_2-TNT/Ti/TNT bifunctional electrode can be described as pseudo-first order kinetics with the rate constant of 1.6×10^{-2} min^{-1}. The method for the preparation of bifunctional electrode provides a very promising environmental technology for water purification and waste effluent treatment.

Keywords: TiO_2 nanotube; β-PbO_2 electrode; electrocatalysis, photocatalysis

1. INTRODUCTION

With the development of industrialization, people's lives have been threatened by all sorts of hazardous materials. Among the hazardous materials, water contaminants have been viewed as the most serious menace to people's lives. Dyeing-weaving wastewater, which is consisted of organic dye such as azo dye, is one of the most common pollutant. In the removal of pollutants from wastewater, a number of methods have been studied including electrochemical oxidation [1], adsorption [2], photocatalytic degradation [3] electrochemical oxidation [4], and photoelectrocatalytic degradation [5], etc. As a process for water purification, photocatalysis has numerous advantages over many existing technologies. The technique can result in the mineralization of pollutants rather than transferring them to an alternative phase, such as is the case with adsorption. Furthermore, photocatalysis does not require the use of hazardous materials such as hypochlorite, peroxide or ozone [6]. In photocatalytic degradation, TiO_2 is considered one of the most promising photocatalysts due to its non-toxic nature, high efficiency, and low cost. However, the TiO_2-based photocatalysts face the problem of the rapid recombination of charge carriers – the photo-generated electrons (e^-) and holes (h^+), which leads to low quantum efficiency. In addition, the recovery and reuse of the photocatalyst has attracted much attention [7]. The photoelectrocatalysis (PEC) method is the most promising alternative in which a bias potential is applied in the photocatalytic degradation using a TiO_2 electrode. The oxidation efficiency was enhanced due to the fact that the applied potential is able to reduce the recombination of photogenerated electron-hole. However, PEC can only be regarded as electro-assisted photocatalysis as the electrocatalysis does not function during this process [8]. Li *et al* [9] fabricated TiO_2 modified PbO_2 electrode and investigated it's performance for photoelectrochemical degradation of methyl blue under visible light irradiation. The results showed that the resulting PbO_2 electrode not only presented excellent photoactivity under visible light irradiation but also a significant synergetic effect in photoelectrochemical processes driven by visible light. Pelegrini *et al* [10] investigated the efficiency of the electrochemically assisted photocatalytic process in the degradation of C. I. Reactive Blue 19 on a $Ti/Ru_{0.3}Ti_{0.7}O_2$ electrode and indicated this combined process permit almost total decolorization of the C.I. Reactive Blue 19 and mineralization of about 50% for a reaction time of 120min.

In some situation, the photoelectrocatalysis is carried out in a annular photoelectrocatalytic reactor, where a irradiation source is placed on the central axis inside the inner tube and the annular TiO_2 electrode is arranged around the inner surface of the outer tube, there has a problem that only one side of TiO_2 electrode can be illuminated by the light, restraining the effectivity of electrode [6]. To tackle this problem, electrochemical catalyst can be coated on the back-lighted side to fabricate the bifunctional electrode, involving an integration of photocatalytic degradation and electrocatalytic oxidation for the pollutant degradation [8,11]. A variety of anode materials including Pt, PbO_2, IrO_2 and SnO_2 electrodes have been extensively investigated [12-14]. Studies show that PbO_2 has electrical conductivity similar to that of metals and it is characterized as a high oxygen evolution potential and low cost [15]. In addition, PbO_2 electrode has a good performance for degradation of organic pollutants, which can be directly oxidized by hydroxyl radicals and chemisorbed active oxygen species generated by electrochemical anodic oxidation [16-18].

Compared with TiO_2 powders and particles, TiO_2 nanotube (TNT) fabricated on the Ti foil has higher specific surface area and better absorption of light [19]. In this work, we report a bifunctional electrode fabricated by combining the TNT photocatalyst with the PbO_2 electrocatalyst. Firstly TiO_2 nanotubes were fabricated on Ti foil by anodic oxidation and then PbO_2 thin film was coated on the opposite side by electrodeposition. To illustrate the catalytic performance of the bifunctional electrode, methyl orange (MO), the most common toxic pollutants in dye wastewater, was chosen as the model pollutant and decolorized by PEC using the resulted bifunctional electrodes. Our investigation demonstrates that the bifunctional electrode shows higher activity for MO decolorization.

2. EXPERIMENTAL

2.1. Materials and chemicals

Titanium foils (about 100μm thick, 99.6%) were purchased from Bao Tai co, Ltd., China. other reagents (analytical grade) were purchased from commercial sources and used without further purification. Twice distilled water was used throughout the experiment.

2.2. Electrode preparation and characterization

Titanium foils were firstly cut into pieces of 5 cm×6 cm and then polished mechanically with sand papers. The titanium plates were degreased by sonication in acetone for 10 min, then washed with pure water, polished chemically in the solution containing hydrofluoric acid (HF): nitric acid (HNO_3): water (H_2O) = 1:4:5 (*V/V*) for about 1-2 min, then completely washed with pure water and finally dried in air. The clean titanium plates were anodized in the solution containing 0.5% ammonium fluoride (NH_4F) and 0.5 mol/L sodium sulfate (Na_2SO_4) by a anodic oxidation process, where a two-electrode electrochemical system with a platinum net as a counter electrode were used. The distance of the two electrodes was 1 cm. The pH was kept at 3 by adding sulfuric acid (H_2SO_4) or sodium hydroxide (NaOH). The voltages were set at 20 V provided by a DC power supply. The anodic oxidation processes were carried out at room temperature for 2 hr. After the anodic oxidation, Ti foils were rinsed with water to remove electrolyte on the surface, the resulted samples were annealed in an oven at 500℃ for 3 hr.

In order to fabricate the bifunctional electrode, the electrocatalyst, PbO_2, was deposited on one side of the double-face TNT electrode by a electrodeposition process. Firstly the prepared TNT electrode with one side being covered with wax was immersed in a quartz tube containing 0.05 mol/L $Pb(NO_3)_2$ and 0.001 mol/L NaF at 30 mA/cm^2 for 60 min. The pH was set at 2 adjusted by HNO_3. Then the resulted electrode was washed with water, immersed in chloroform ($CHCl_3$) to remove the wax, and dried in air. Finally the bifunctional electrode was obtained and labelled as PbO_2-TNT/Ti/TNT.

Morphology of the electrode was characterized by scanning electron microscopy (SEM) (JEOL 6360LV and FEI Qaunta 200) with an acceleration voltage of 10 kV and 30 kV. The X-ray diffraction (XRD) patterns were recorded on a D8 Advance X-diffractometer (Cu $K\alpha$, $\lambda = 0.15406$ nm) (Bruker, Germany).

2.3. Cyclic voltammetry measurement of the electrode

A three-electrode system was used to measure cyclic voltammetry curves of the bifunctional electrode. The fabricated bifunctional electrode was chosen as the work electrode with the effective area of 9 cm^2, a Pt grid as the counter electrode and Ag/AgCl electrode as the reference electrode. The electrochemical work station (RST-3000, Resitest Instrument Technology Co., Ltd, China) was used to record the cyclic voltammetry curves of the bifunctional electrode at scanning rate of 20 mV/s in the sulfuric acid solution of 0.5 mol/L. The measurement was pre-polarized for 20 min at the current density of 50 mA/cm^2. All measurements were carried out at room temperature.

2.4. Photoelectrocatalytic test

In the PEC measurements, a 500 W parallel xenon lamp light source (CHF-XM35-500W, Trusttech Science and Technology Co., Ltd, China) was used to simulate the sunlight and a electrochemical work station (RST-3000, Resitest Instrument Technology Co., Ltd, China) was employed to provide the bias potential. A three-electrode system, consisting of the bifunctional electrode as the working electrode, a platinum grid as the counter electrode and Ag/AgCl electrode as the reference electrode, was used for the decolorization of methyl orange (MO). The solution contained 0.1 mol/L $NaNO_3$ and its pH was adjusted with HNO_3 and NaOH. The decolorization time was maintained for 3 hr. The concentration of MO was determined by measuring the UV-visible adsorbance of 4.0 mL sample taken from the solution every 30 min. After measurement, the sample was put back to the reaction solution to keep the volume constant. For the comparison, the electrocatalytic (EC) performance on the bifunctional electrode was also investigated.

3. RESULTS AND DISCUSSION

3.1. Bifunctional electrode characterization

The morphologies of the fabricated electrodes are shown in Figure 1. It can be seen that the PbO_2 films have uniform micro-structures, compacted particles and no obivous cracks between the crystal particles. The PbO_2 electrode has pyramid-shaped morphologies. The images of the TiO_2 nanotube side are shown in Figure 1c and 1d. It is observed that highly ordered, self-assembled TiO_2 nanotubes have been formed. The TiO_2 nanotubes have a pore diameter ranging from 70 to 100 nm with a wall thickness of about 6 nm and the tube length ranging from 443 nm to 480 nm.

The XRD patterns of PbO_2-TNT/Ti/TNT bifunctional electrodes are shown in Figure 2. As shown in Figure 2a, on the side of TiO_2 nanotubes several remarkable peaks at 35.46°, 38.77°, 40.52°, 53.31°, 63.26°, 70.96° are attributed to the Ti substrate (JCPDS 65-6231).

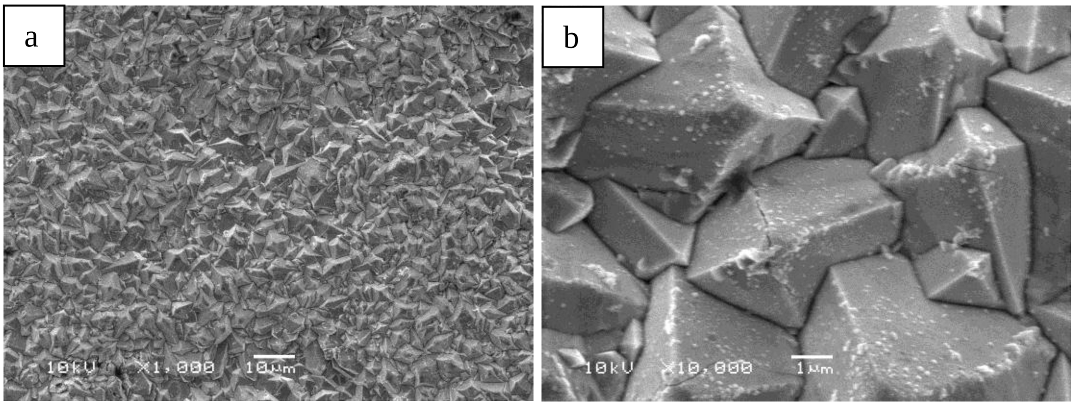

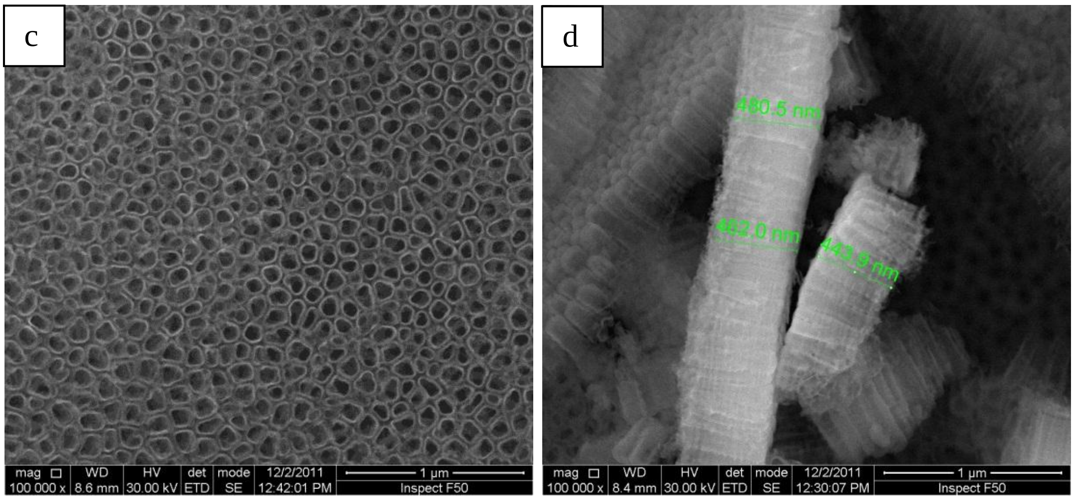

Figure 1. SEM images of the bifunctional electrod prepared at current density of 30 mA/cm^2 for 60 min. (a), (b) the sorface of PbO_2 film, the surface (c) and the cross-section (d) of TiO_2 nanotubes

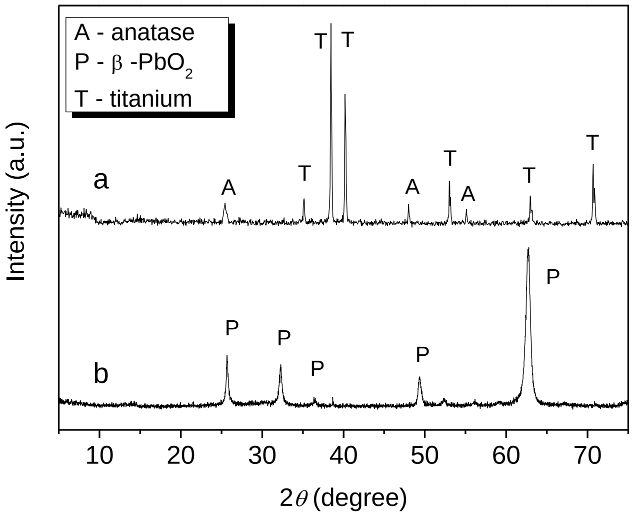

Figure 2. XRD pattern of PbO_2-TNT/Ti/TNT electrode. (a) the side of TiO_2 NT, (b) the side of PbO_2-TNT

The weak peaks at 25.3°, 48.1° and 55.2° belong to anatase (PDF 21-1272). The intensity of these three peaks is weak due to relative thin TiO_2 nanotube layer. Figure 2b shows that some peaks at 25.650°, 32.281°, 36.514°, 49.350°, and 62.76° present in the XRD pattern for the PbO_2 side. These peaks are attributed to β-PbO_2 (PDF 41-1492). Other phases of PbO_2 are not found in the XRD pattern.

3.2. Cyclic voltammetry

CV measurements were used to investigate the electrochemical performance of the bifuctional electrodes. Figure 3 presents the cyclic voltammogram of the prepared PbO_2-TNT/Ti/TNT electrode in 0.5 M H_2SO_4 solution at a scan rate of 20 mV/s. It can be found that anodic current peak is at about

1.40 V and cathodic current peak is at about 0.80 V, representing the oxidation and reduction of Pb(IV)/Pb(II)/Pb(0) couples [20]. Further scanning the potential above 1.7 V, the electrochemical current undergoes a rapid linear increase due to oxygen evolution.

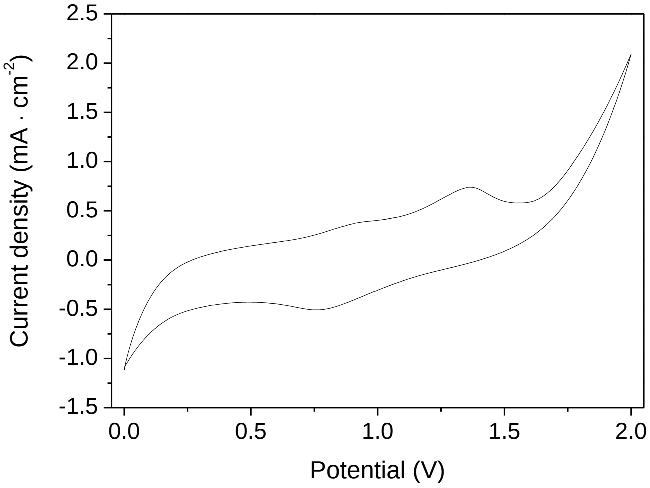

Figure 3. The cyclic voltammetry curve of PbO_2-TNT/Ti/TNT electrode in 0.5 mol/L H_2SO_4 solution at a potential scan rate of 20 mV/s

3.2. Decolorization of MO on electrodes

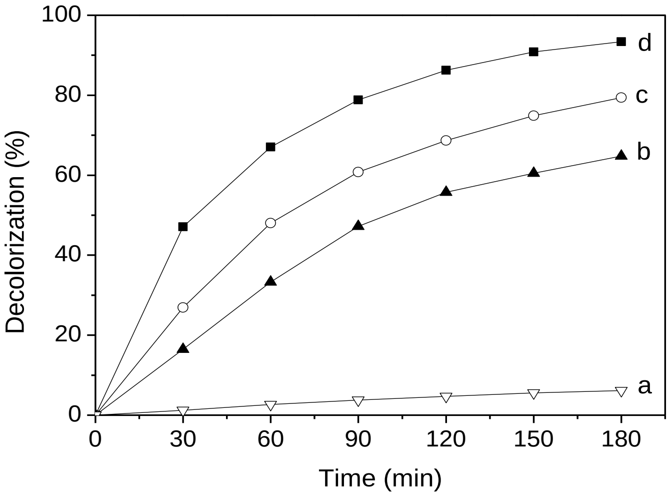

Figure 4. The decolorization of MO by EC process on Ti/TNT (a), PbO_2-TNT/Ti/TNT (b) electrodes and PEC processe on Ti/TNT (c), PbO_2-TNT/Ti/TNT electrodes (d)

To investigate the catalytic performance of the fabricated bifunctional electrode, MO was used as a model pollutant in the test. Figure 4 presents the decolorization of MO by PEC and EC on Ti/TiO_2 nanotube monofunctional electrode and PbO_2-TNT/Ti/TNT bifunctional electrode. The initial concentration of MO was 10 mg/L and pH was controlled at 3.

For the photocatalysis process on the TiO_2-based catalyst, it is known that the strong oxidant, photogenerated holes could oxidize water adsorbed on the TiO_2 nanotube surface to create the strong oxidizing agent hydroxyl radical. Both the photogenerated holes and hydroxyl radical could oxidize organic compounds as represented by Eqs. (1)–(4).

$$\mathrm{TiO_2} + h\nu \rightarrow h^{+} + e^{-} \qquad (1)$$

$$\mathrm{TiO_2} + h^{+} + \mathrm{H_2O} \rightarrow \mathrm{TiO_2[OH\bullet]} + \mathrm{H^{+}} \qquad (2)$$

$$h^{+} + \mathrm{R} \rightarrow \mathrm{R\bullet} \qquad (3)$$

$$\mathrm{TiO_2[OH\bullet]} + \mathrm{R} \rightarrow \mathrm{TiO_2} + \mathrm{RO} + \mathrm{H^{+}} + e^{-} \qquad (4)$$

When an extra potential is applied, the photogenerated electrons transferred to external circuit (counter electrode) at a given applied potential. This transportation effectively prevents the recombination of photogenerated electrons and holes. The photo-current increased with potential bias and then reached saturation gradually owing to the transportation and production of photogenerated electrons reached equilibrium [21]. Furthermore, The generated photoelectrons at counter electrode (Pt grid in our case) can react with dissolved oxygen molecules and produce oxygen peroxide radicals $O_2\bullet^{-}$, which is also powerful oxidizing agents capable of degrading most pollutants [10].

$$\mathrm{e^{-}} + \mathrm{O_2} \rightarrow \mathrm{O_2\bullet^{-}} \qquad (5)$$

$$\mathrm{O_2\bullet^{-}} + \mathrm{R} \rightarrow \mathrm{O_2} + \mathrm{RO} + \mathrm{H^{+}} + e^{-} \qquad (6)$$

For the electrochemical oxidation on the PbO_2 surface, anodic discharge of water at the active site produces absorbed hydroxyl radicals ($PbO_2(OH\bullet)$), which can oxidize organic compounds. The reactions can be shown as:

$$\mathrm{PbO_2} + \mathrm{H_2O} \rightarrow \mathrm{PbO_2(OH\bullet)} + \mathrm{H^{+}} + \mathrm{e^{-}} \qquad (7)$$

$$\mathrm{PbO_2[OH\bullet]} + \mathrm{R} \rightarrow \mathrm{PbO_2} + \mathrm{RO} + \mathrm{H^{+}} + e^{-} \qquad (8)$$

The electrochemical-assisted photocatalysis process is illustrated in Figure 5.

When the applied potential is higher, more hydroxyl radicals are produced and the electrochemical oxidation activity increases. However, significant quantities of hydrogen peroxide are expected to be formed by combining the absorbed hydroxyl radicals with each other. Afterward, further anodic oxidation to oxygen (oxygen evolution reaction) may occur, competing with the reaction of pollutant mineralization simultaneously, as shown in the following equation [22]:

$$OH\bullet + OH\bullet \rightarrow H_2O_2 \rightarrow O_2 + H^+ + e^- \quad (9)$$

In EC test, 1.4 V potential was added on the working electrodes, and no light was illuminated. It is shown that after the three-hour test on Ti/TiO_2 nanotube monofunctional electrode without illuminating by Xenon lamp in EC test, the decolorization of MO only increases slightly (about 6 %), indicating that the EC activity of TiO_2 nanotube is low.

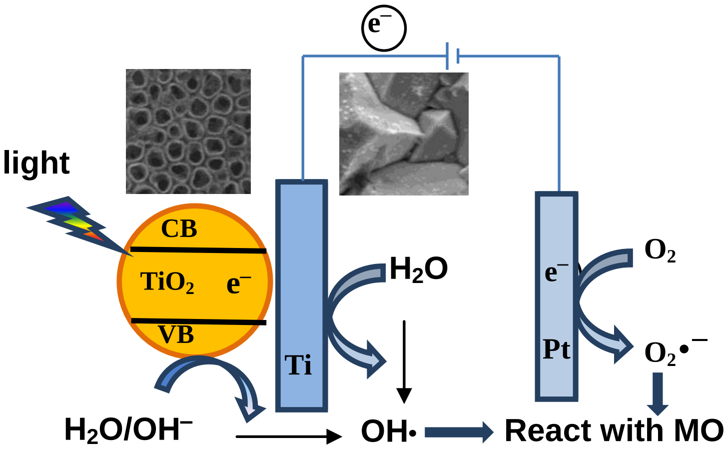

Figure 5. Schematic mechanism for the electrochemical assisted photocatalysis on PbO_2-TNT/Ti/TNT electrode

While the MO decolorization by EC on PbO_2-TNT/Ti/TNT electrode is remarkable higher than that on Ti/TiO_2 nanotube electrode at the same EC conditions, showing the modification of PbO_2 provided a better EC activity. The increase in decolorization value on PbO_2-TNT/Ti/TNT bifunctional electrode by EC is about 59 %. In the PEC process, besides the bias potential was applied on the working electrode, the illumination from Xenon lamp was also used. This combination gives MO decolorization of approximately 80 % on Ti/TiO_2 nanotube monofunctional electrode, while about 93 % of MO is decolorized on PbO_2-TNT/Ti/TNT bifunctional electrode. For the monofunctional Ti/TiO_2 nanotube electrode, the applied potential just took part in the separation of photogenerated electrons (e^-) and holes (h^+), but for the PbO_2-TNT/Ti/TNT bifunctional electrode, it also promoted the electrocatalysis on PbO_2 electrode. This synergetic effect resulted in the higher decolorization of MO. This synergism can be explained in term of: (1) in the presence of high energy photons the external bias can contribute to the diminution of the electron–hole par recombination process. (2) The photons reaches the electrode surface during electrochemical steps and can form excited radicals which can enhance the dye degradation [23].

It was reported that the decolorization of MO can be described as pseudo-first order kinetics [24]. The Langmuir–Hinshelwood pseudo-first order kinetic model can be expressed by the following equation:

$$\ln(\frac{C_0}{C_t}) = k_{app}t \qquad (1)$$

where C_t is the concentration of the reactant at t time, C_0 the initial concentration of the reactant and k_{app} is the apparent rate constant.

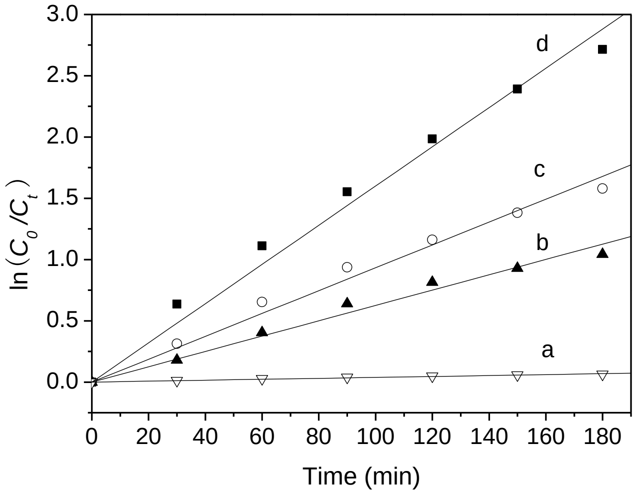

Figure 6. Plots of the ln(C_0/C_t) *vs* *t* for the degradation of MO. The experimental conditions are the same as described in Figure 4

Figure 6 presents the corresponding ln(C_0/C_t) *vs* *t* plots for the tests reported in Figure 4. The linear relationship of ln(C_0/C_t) *vs* *t* shows that the degradation of MO using either the monofunctional or bifunctional electrodes follows pseudo-first order kinetics. The pseudo-first order kinetics parameters (K_{app}) of decolorization processes are presented in Table 1.

Table 1. Kinetics parameters for different decolorization processes

Decolorization process	K_{app} ($\times 10^{-3}$ min^{-1})	R^2
EC on TiO_2 nanotube electrode	0.38	0.9808
EC on PbO_2-TNT/Ti/TNT electrode	6.25	0.9808
PEC on TiO_2 nanotube electrode	9.33	0.984
PEC on PbO_2-TNT/Ti/TNT electrode	16.00	0.9838

The TiO_2 nanotube electrode under the applied electrode potential of 1.4 V but without any light illumination has the lowest electrochemical degradation rate constant, 3.8×10^{-4} min^{-1} (Plot *a*). As shown in Plot *b*, when the same potential is applied on the PbO_2-TNT/Ti/TNT bifuctional electrode, the degradation rate constant of MO approaches to 6.25×10^{-3} min^{-1}, which is much larger than that of Plot *a*, demonstrating that the PbO_2 has the better electrochemical oxidation performance for MO. As shown in Plot *c*, the PEC on the monofunctional TiO_2 nanotube electrode at the applied potential of 1.4 V gives a rate constant of 9.33×10^{-3} min^{-1}. Among the four plots, Plot *d*, for the PbO_2-

TNT/Ti/TNT bifunctional electrode at the applied potential of 1.4 V and under the light illumination, has the highest slope, 1.6 $\times 10^{-2}$ min^{-1}, which is about 1.7 times larger than that of Plot *c*. The above results demonstrate the benefits of the combination of photocatalytic degradation and electrochemical oxidation for the degradation of organic pollutants.

3.3. The effect of appliad potential

To investigate the dependence of MO decolorization from the oxidation on bias potential for the electrode, an array of control experiments by PEC were performed using PbO_2-TNT/Ti/TNT bifunctional electrode, the obtained results are shown in Figure 7.

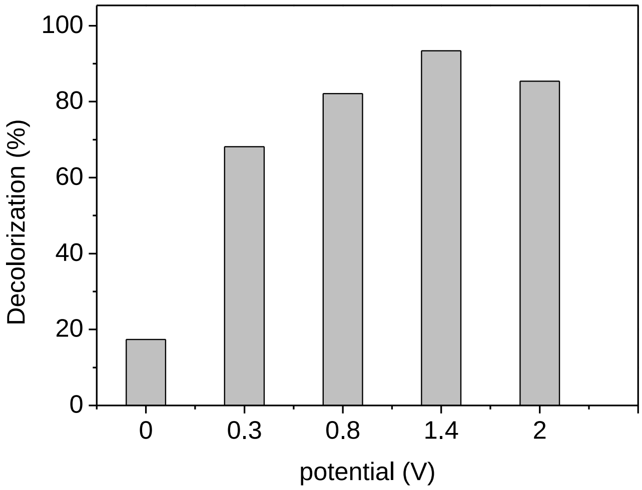

Figure 7. The influence of bias voltage on the decolorization of MO

It can be found that when no applied potential is added to the electrode, MO is decolorized only by photo-oxidation and the decolorization is relative low, owing to the combination of photogenerated electrons and holes. When the potential of 0.3 V is applied on the working electrode, the MO decolorization increases because of the effective suppression of recombination between the photogenerated electrons and holes. Further increasing the potential up to 1.4 V, the higher applied potential not only effectively promoted the separation of photogenerated electrons and holes, but also drove the production of hydroxyl radicals on PbO_2 electrode, as a result the MO decolorization increases. When the potential exceeds 1.4 V, the oxygen evolution reaction was more obvious, which caused the decrease of the MO decolorization [10].

3. CONCLUSIONS

In summary, a bifunctional electrode with TiO_2 nanotube on one side and PbO_2 on the reverse side was fabricated for the decolorization of MO. Compared with the monofunctional Ti/TiO_2 NT electrode, the PbO_2-TNT/Ti/TNT bifunctional electrode shows higher PEC performance for the decolorization of MO, due to both photocatalysis and electrocatalysis were carried out at the same time and they were synergistic. This photoelectro-synergistic catalysis process should be operated at a suitable applied potential which is no more than oxygen evolution potential. The MO decolorization of 93% was obtained at the applied potential of 1.4 V. The degradation rate constant for this bifunctional electrode is about 1.7 times larger than that for monofunctional electrode. The method for the preparation of bifunctional electrode with both photo- and electro-catalytic performance provides a very promising environmental technology for water purification and waste effluent treatment.

ACKNOWLEDGMENTS

The authors gratefully acknowledge the financial support for this work from the Education Office of Liaoning Province, China (Project No. LS 2010121) and Science and Technology Bureau of Shenyang, China (Project No. F10-205-1-61). The work was also supported by the project on Scientific Research for Public Interest of Liaoning Province (Project No. 2011001001), China.

References

1. I. Sirés, C.T.J. Low, C. Ponce-de-León and F.C. Walsh, *Electrochem. Commun.*, 12(2010)70
2. M.H. Zhang, Q.L. Zhao and Z.F. Ye, *J. Environ. Sci.*, 23(2011) 1962
3. A. Kar, Y.R. Smith and V. Subramanian, *Environ. Sci. Tech.*, 43(2009) 3260
4. M. Zidan, T.W. Tee, A.H. Abdullah, Z. Zainal, and G. J. Kheng, *Int. J. Electrochem. Sci.*, 6 (2011) 279
5. H. Xu, Q. Zhang, W. Yan and W. Chu, *Int. J. Electrochem. Sci.*, 6(2011) 6639
6. C. McCullagh, N. Skillen, M. Adams and K.J. Robertson Peter, *J. Chem. Tech. Biot.*, 86(2011) 1002
7. G.T. Li, H.Y. Yip, K.H. Wong, C. Hu, J.H. Qu and P.K. Wong, *J. Environ. Sci.*, 23(2011) 998
8. X. Qu, M. Tian, S. Chen, B.Q. Liao and A.C. Chen, *Electroanal.*, 23(2011) 1267
9. G.T. Li, H.Y. Yip, K.H. Wong, C. Hu, J.H. Qu, and P.K. Wong, *J. Environ. Sci.*, 23(2011) 998
10. R. Pelegrini, P. Peralta-Zamora, A.R. de Andrade, J. Reyes and N. Durán, *Appl. Catal. B Environ.*, 22(1999)83
11. R.M. Asmussen, M. Tian and A.C. Chen, *Environ. Sci. Technol*, 43(2009)5100
12. M.H. Zhou and J. J. He, *J. Hazard. Mater.*, 153(2008)357
13. G.H. Zhao, J.X. Gao, W. Shi, M.C. Liu and D.M. Li, *Chemosphere*, 77(2009)188
14. L. H. Tran, P. Drogui, G. Mercier and J. F. Blais, *J. Environ. Eng.*, 135(2009)1051
15. J.J. Wei, X.P. Zhu, F.X. Lu and J.R. Ni. *Int. J. Min. Met. Mater.*, 18(2011)589
16. M.H. Zhou, Q.Z. Dai, L.S. Lei, Z.C. Wu, C.A. Ma and D.H. Wang, *Acta Phys.-Chim. Sin.*, 20(2004) 871
17. S.P. Tong, C.A. Ma and H. Feng, *Electrochim. Acta*, 53(2008)3002
18. F. Fu, W.H. Yang and H. H. Wang, *J. Inorg. Mater.*, 25(2010)653
19. D. Gong, C.A. Grimes and O.K. Varghese, *J. mater. Res.*, 16(2001) 3331
20. Z.Q. He, C.X. Huang, Q. Wang, Z. Jiang, J.M. Chen, and S. Song, *Int. J. Electrochem. Sci.*, 6(2011) 4341
21. J. Li, L. Zheng, L. Li, G. Shi, Y. Xian and L. Jin, *Talanta*, 72 (2007) 1752
22. G.H. Chen, *Sep. Purif. Technol.*, 38(2004)11
23. S.Q. Wei, Z.C. Shao, X.D. Lu, Y. Liu, L.L. Cao and Y. He, *J. Environ. Sci.*, 21(2009)991